

RSC Advances



This is an *Accepted Manuscript*, which has been through the Royal Society of Chemistry peer review process and has been accepted for publication.

Accepted Manuscripts are published online shortly after acceptance, before technical editing, formatting and proof reading. Using this free service, authors can make their results available to the community, in citable form, before we publish the edited article. This *Accepted Manuscript* will be replaced by the edited, formatted and paginated article as soon as this is available.

You can find more information about *Accepted Manuscripts* in the [Information for Authors](#).

Please note that technical editing may introduce minor changes to the text and/or graphics, which may alter content. The journal's standard [Terms & Conditions](#) and the [Ethical guidelines](#) still apply. In no event shall the Royal Society of Chemistry be held responsible for any errors or omissions in this *Accepted Manuscript* or any consequences arising from the use of any information it contains.

Copolymers from epoxidized soybean oil and lactic acid oligomers for pressure-sensitive adhesives

Yonghui Li^a, Donghai Wang^b, Xiuzhi Susan Sun^{a,*}

^aBio-Materials and Technology Lab, Department of Grain Science and Industry, Kansas State University, Manhattan, KS 66506

^bDepartment of Biological and Agricultural Engineering, Kansas State University, Manhattan, KS 66506

*Correspondence to: Xiuzhi Susan Sun, E-mail: xss@ksu.edu, Phone: 785-532-4077, fax: 785-532-7193

Submitted to *RSC Advances*

Abstract:

Plant oils and polysaccharide-derived lactic acid are two renewable chemicals that are important in producing industrial biopolymers. In this investigation, we copolymerized epoxidized soybean oil (ESO) with lactic acid oligomers for pressure-sensitive adhesive (PSA) applications. Lactic acid oligomers (OLAs) with molecular weights of 260 to 674 g/mol were synthesized without catalysts or solvents. Both carboxyl and hydroxyl groups of OLAs are able to open the epoxide ring of the ESO triglycerides to form polymer networks. Thermal, mechanical, and viscoelastic properties of the copolymers were studied for potential applications as single-component pressure-sensitive adhesives (PSAs). Glass transition temperatures (T_g) of copolymers increased from -21 to 5 °C as chain lengths of OLAs increased. Copolymers based on relatively short-chain OLAs exhibited maximal peel adhesion strength of 3.8 N/cm, tack adhesion of 8.0 N/cm, and shear adhesion resistance of over 30,000 minutes. We also found positive correlations between mechanical performance and viscoelastic response at bonding and debonding frequencies for these copolymers. The new polymers are favorable candidates for fully biobased PSAs.

Key words:

Epoxidized soybean oil, lactic acid oligomers, UV polymerization, pressure-sensitive adhesives (PSA), biobased product

Introduction

A pressure-sensitive adhesive (PSA) adheres instantly to a variety of substrates under light pressure (e.g., finger pressure) without chemical changes or activation¹. The strength of an adhesive bond is determined by the thermodynamic contributions of interfacial energy (e.g., van der Waals interaction, electrostatic forces, and hydrogen bonding) and the rheological contributions of the adhesive layer itself². The unique design of PSAs provides enough potential deformability and wettability to achieve contact with substrates yet sufficient internal strength (i.e., cohesion) to resist deformation. PSAs can be single-component (i.e., single polymer) and multi-component types (i.e., elastomer plus tackifier and other additives). PSAs are made predominately from petrochemicals, such as acrylics, silicones, synthetic polyisoprene, polybutadienes, and various copolymers¹. Developing PSA resins from renewable bio-resources is economically attractive and socially responsible³⁻⁶.

Plant oils are one of the most attractive renewable resources because of their universal availability, biodegradability, relatively low cost, and superb environmental credentials (i.e., low ecotoxicity and low toxicity toward humans)⁷. They are mixtures of triglycerides with varying compositions of saturated and unsaturated fatty acids, depending on the crop, season, and growing conditions⁸. The reactive sites of triglycerides (e.g., double bonds, ester groups) enable various possibilities for tailoring new structures, such as fatty acids, diols, diacids, epoxides, or polyols, as well as well-defined linear polymers and 3D networks⁹⁻¹¹. These derivatives have found practical

applications in resins, composites, coatings, adhesives, surfactants, lubricants, cosmetic products, and biomedical uses^{7, 12}.

Recent efforts have been made to develop PSAs from plant oils, and several chemical pathways have been explored. Wool and coworkers synthesized polymers from acrylated methyl oleate and copolymers with other petrochemical acrylates through emulsion polymerization^{5, 13, 14}. The polymers exhibited relatively good tack and peel properties, but their shear resistance was weak. Li and colleagues polymerized a mixture of epoxidized fatty acids in the presence and absence of dicarboxylic acid under heat with trivalent organic chromium complexes as catalysts¹⁵, but shear resistance of the adhesives was only a few hours. Koch et al. proposed that PSAs could be developed through the polymerization of epoxidized or acrylated triglycerides and fatty acids or copolymerization with alcohols or amines, but adhesion performance was not reported in the patent application^{16, 17}. Sun and co-workers previously developed PSAs from epoxidized soybean oils (ESO) and dihydroxyl soybean oils through hot-air curing in the presence of a phosphoric acid catalyst and UV curing with a cationic photoinitiator¹⁸⁻²⁰. The PSAs exhibited good peel and tack performance and excellent shear resistance (> 10,000 minutes). The UV-PSA is a multi-component system with rosin ester tackifiers to adjust the viscoelasticity and improve adhesion.

In this research, we studied lactic acid as another alternative resource for PSA application. Lactic acid (LA) is a commercially available chemical that is produced primarily through the fermentation of renewable polysaccharides (e.g., starch, cellulose). Oligomerization and polymerization of LA occur in the absence of catalysts via a condensation reaction,

which offers an economical viable pathway. Molecular weight can be controlled easily by adjusting reaction parameters (e.g., times, temperatures, and vacuum levels)²¹. Lactic acid oligomers are bifunctional compounds with a carboxylic acid group at one end and a hydroxyl group at the other. Both carboxyl and hydroxyl groups are able to open the epoxide ring of triglycerides with the appropriate catalysts to form polymer networks. The objectives of this study were to develop copolymers from epoxidized soybean oils and lactic acid oligomers (OLA) and to evaluate the thermal, mechanical, and viscoelastic properties of the copolymers for potential applications as single-component PSAs. OLAs with varied chain length were synthesized through a melt-condensation reaction without any catalyst and solvent, and the copolymers were synthesized via a cationic UV polymerization approach.

Experimental

Materials

ESO (VIKOFLEX 7170, epoxy oxygen content 7.0%, corresponding to 4.3 epoxide groups per triglyceride molecular) was provided by Arkema Inc. (King of Prussia, PA). PC-2506 (diaryliodonium hexafluoroantimonate) was used as a cationic photo initiator and obtained from Polyset Company (Mechanicville, NY). L-(+)-Lactic acid (LA) was supplied as a 90 wt% aqueous solution by Sigma-Aldrich (St. Louis, MO) and used as received. All other chemicals were purchased from Fisher Scientific (Waltham, MA).

Synthesis of lactic acid oligomers (OLAs)

200 g LA aqueous solution was charged into a three-necked flask equipped with a mechanical stirrer and a reflux condenser that was connected with a vacuum system through a liquid nitrogen cold trap. The solution was first dehydrated at 110 °C in an oil bath under atmospheric pressure for 2 h. The temperature was raised gradually to 160 °C, then pressure was reduced gradually (over 4 h) to 30 torr. The reaction was then continued at 160 °C/10 torr. Samples were collected at different post-reaction times (1 h, 3 h, 5 h, and 7 h) to obtain OLAs with varied chain length (i.e., degree of polymerization). OLAs were designated OLA3, OLA5, OLA7, and OLA9 according to their degrees of polymerization.

Characterization of OLAs

The molecular weight (MW) of OLAs was determined through carboxyl end group titration²². Approximately 1 g of OLA was accurately weighted and dissolved in 20 ml dichloromethane/methanol (1:1 volume ratio). The dissolved sample was titrated with 0.5 N sodium methoxide solution in methanol using bromothymol blue as indicator. Degree of polymerization (DP) was calculated based on MW according to equation (1) below:

$$DP = \frac{MW-18}{72} \quad (1)$$

Glass transition temperatures (T_g) of OLAs were measured with a TA Q200 differential scanning calorimetry (DSC) instrument under nitrogen atmosphere (TA Instruments, New Castle, DE). About 10 mg OLA was accurately weighed and sealed in a stainless steel pan, and an empty pan was used as a reference. The sample was heated from -80 °C to 150 °C at a rate of 10 °C/min. Thermal stability of OLAs was measured with a

PerkinElmer Pyris1 thermogravimetric analyzer (TGA). About 10 mg OLA was placed in a platinum pan and heated from 40 °C to 700 °C at a heating rate of 20 °C/min under a nitrogen atmosphere.

Fourier transform infrared spectroscopy (FTIR) spectra of OLAs were acquired with a PerkinElmer Spectrum 400 FT-IR/FT-NIR Spectrometer (PerkinElmer, Shelton, CT). Spectra of 32 scan from each sample were collected in the region of 4000 to 400 cm^{-1} with a spectral resolution of 1 cm^{-1} .

Synthesis of ESO/OLA copolymers

Three different molar ratios of OLA to ESO (2.5, 3, and 3.5) were used for the copolymer with each OLA to gauge the influence of both OLA amounts and DP on polymer properties and PSA performance. Such OLA to ESO ratios corresponded to hydroxyl and carboxyl groups to epoxides molar ratios of 1.16, 1.39, and 1.63 in the copolymer formulation, respectively. The amount of photoinitiator was fixed at 3% based on the weight of ESO. Formulated ESO/OLA/photoinitiator was thoroughly mixed in a 25-mL glass vial with the aid of heat gun, Vortex mixer, and sonicator. The mixture was then coated onto PET film using an EC-200 Drawdown Coater with #6 coating bar (Chem Instruments Inc., Fairfield, OH). The coating amount was calculated to be 14.58 g/m^2 . The coated resin was polymerized with a Fusion 300S 6'' UV system (300 W/inch power, D bulb, UVA radiation dose 215-231 mJ/cm^2) equipped with an LC6B benchtop conveyor at conveyor speed of 7 ft/minute. The cured copolymers based on OLA3 were designated OLA3P1, OLA3P2, and OLA3P3, with molar ratios of OLA3 to ESO of 2.5, 3, and 3.5, respectively. The cured copolymers based on OLA5 were designated OLA5P1,

OLA5P2, and OLA5P3, with molar ratios of OLA5 to ESO of 2.5, 3, and 3.5 respectively. Copolymers based on OLA7 and OLA9 were similarly designated.

Model system design and characterization

In order to better understand the reaction between ESO and OLA, we used epoxidized methyl oleate (EMO, 0.97 oxirane) as a model representative of ESO and lactic acid (LA) (>98%, Sigma) as a representative of OLAs. Same molar amount of EMO and LA were reacted in the presence of PC-2506. The product (EMOLA) was purified through ether extraction and washed with water to eliminate the initiator and excess lactic acid. The organic phase was dried over anhydrous magnesium sulfate then filtrated and concentrated under vacuum. The samples were characterized with FTIR (PerkinElmer Spectrum 400 Spectrometer, 4000 to 400 cm^{-1} , 32 scans).

Characterization of ESO/OLA copolymers for PSAs

Glass transition and thermal stability of copolymers were measured with a Q200 DSC and Pyris 1 TGA, respectively. Copolymers used for measurements were carefully scratched from PET backing with a blade. The methods were the same as those previously described for OLAs.

The PET films coated with copolymer layers were cut into 2.54cm \times 12.7cm strips. The peel strength was measured following ASTM D3330²³, and loop tack strength was measured following ASTM D6195²⁴ with an IMADA MV-110-S tester (Imada Inc., Northbrook, IL) on 18-gauge, 304 stainless-steel test panels (ChemInstruments, Inc., Fairfield, OH) with a stressing clamp moving speed of 5.0 mm/s. Five specimens were

measured for each formulation. The shear test was conducted following ASTM D3654²⁵ using a Room Temperature 10 Bank Shear (ChemInstruments, Inc., Fairfield, OH) with 2.54cm × 2.54cm specimens and test mass of 1000 g on 18-gauge, 304 stainless-steel test panels. The time between the application of the load to the specimen and its separation from the panel was recorded. Three replicates were conducted for each sample.

Viscoelasticity of copolymers was measured using a Bohlin CVOR 150 rheometer (Malvern Instruments, Southborough, MA) with a PP 20 parallel plate in shear mode. The specimen was taped to the stationary base of the rheometer with the adhesive side facing the parallel plate probe. The gap was closed with normal force. The strain amplitude was set at 0.1%, and oscillatory frequency sweep was performed from 0.01 to 100 rad/s. Storage modulus (G') and loss modulus (G'') as a function of frequency were recorded to show how the adhesives responded at different timescales. Dynamic mechanical analysis (DMA) of selected copolymers was conducted using a TA Q800 DMA analyzer equipped with a liquid nitrogen cooling system in a shear sandwich mode at 1 Hz frequency and 0.1% strain (linear viscoelastic region). Specimens (about 10 mm × 10 mm × 1 mm) were cut from a non-supported copolymer sheet with a blade and heated from -120 to 120 °C at a rate of 3 °C/min under a nitrogen atmosphere. Crosslink density (ν_e) and molecular weight between cross-links (M_c) of the copolymer was estimated from DMA data according to equations (2) and (3):²⁶

$$\nu_e = \frac{G'}{RT} \quad (2)$$

$$M_c = \frac{\rho}{\nu_e} \quad (3)$$

where G' is the shear storage modulus of the cross-linked polymer in the rubbery plateau region 50 °C above $\tan\delta$ peak temperature, R is the gas constant, T is the corresponding absolute temperature, and ρ is the specific gravity of the copolymer.

Gel content of selected copolymers was measured by immersing the sample in a large amount of toluene²⁷. Approximately 0.2 g of copolymer sheet was accurately weighed and immersed in 20 mL toluene for 1 week. The specimen was then taken out and dried at 130 °C for at least 2 hours until a constant weight was achieved. Gel content was measured according equation (4) below:

$$\text{Gel content} = w_1/w_0 \times 100 \quad (4)$$

where w_0 and w_1 are the weights before and after toluene soaking, respectively.

Results and discussion

Properties of OLAs

Four types of OLAs were synthesized: OLA3, OLA5, OLA7, and OLA9. Their MW were determined to be 260, 398, 568, and 674 g/mol, respectively, corresponding to a DP of 3.4, 5.3, 7.6, and 9.1 (Table 1). OLAs with DP larger than 9 were not used in this study, because viscosity and T_g increased greatly as chain length increased further, which limited subsequent processing and formulation for UV polymerization.

The four OLAs exhibited similar FTIR absorption spectra (Figure 1), with the exception of variations in the 1700-1750 cm^{-1} region (Figure 1 insert), which corresponded to stretching vibration of carbonyl groups (C=O). The C=O bands of OLA3, OLA5, OLA7, and OLA9 were observed at 1740, 1744, 1746, and 1748 cm^{-1} , respectively, and the intensity increased as OLA chain length increased. The position of C=O varied slightly

by compound. The band of C=O of carboxyl groups of lactic acid appeared at 1720 cm^{-1} ²⁸, whereas that of the ester group of high-molecular-weight poly(lactic acid) appeared at 1750 cm^{-1} ²⁹. Longer-chain OLAs contained more ester groups and fewer carboxyl groups, resulting in a blue shift in the absorption peak. Other OLA band assignments can be found in the literature²⁸.

The T_g of OLAs increased from $-24.3\text{ }^\circ\text{C}$ to $8.9\text{ }^\circ\text{C}$ as molecular weight increased from 260 to 674 g/mol (Figure 2, Table 1). Generally, T_g increases with molecular weight then reaches a moderate molecular weight point after which further increase in molecular weight has little effect on T_g . This dependence is explained by the free-volume theory of glass transition: because large free volume is associated more with the ends of long polymer chains than with other chain segments, free volume increases with an increasing number of chain ends (i.e., decreasing molecular weight).

The OLAs exhibited a two-stage decomposition profile (Figure 3). First-stage weight loss was attributed to the evaporation and decomposition of volatiles and low-molecular-weight components (e.g., lactic acid, lactide) in the OLAs, whereas second-stage weight loss was caused by the decomposition reaction of oligomer backbones. The main decomposition products included carbon dioxide, acetaldehyde, ketene, carbon monoxide, lactide, etc., as reported in the literature.³⁰ Decomposition temperature at peaks ($T_{d, \max}$) increased as OLA chain length increased (Table 1); for example, the $T_{d, \max}$ of OLA3 was $278.2/375.2\text{ }^\circ\text{C}$, whereas the $T_{d, \max}$ of OLA7 increased to $309.2/382.3\text{ }^\circ\text{C}$. Takizawa also reported that the decomposition temperatures of lactic acid oligomers increased gradually as chain length increased from 1 to 64 repeating units³¹.

ESO/OLA copolymerization and model compounds study

OLAs are bifunctional compounds with a carboxylic acid group at one end and a hydroxyl group at the other. Both carboxyl and hydroxyl groups of organic compounds are able to open the epoxide ring on fatty acids with an appropriate catalyst³²⁻³⁵. During UV polymerization, the photoinitiator (diaryliodonium salt) absorbed UV light and decomposed into long-lived superacid. The superacid further catalyzed the step-growth polymerization of ESO and OLAs to form hydroxyl functionalized polyesters and polyethers via the ring opening of epoxy groups with –COOH and –OH in OLAs, as well as epoxides homopolymerization and polymerization of remaining epoxides with newly formed hydroxyl groups (Figure 4). Through UV polymerization, viscous liquid resins were converted into high-molecular-weight viscoelastic adhesives.

Typical FTIR spectra of model compounds (EMO and LA) and product (EMOLA) were presented in Figure 5. EMO exhibited characteristic oxirane peak (ν_{C-O-C}) at 826 and 846 cm^{-1} , which were completely disappeared in EMOLA, indicating successful ring-opening of ESO with LA. New OH peak at 3480 cm^{-1} was observed in EMOLA. Furthermore, several new peaks attributed to the backbone of LA were also noticed in EMOLA, including 1416 cm^{-1} (ν_{CO} and δ_{OH} of acid group), 1373 cm^{-1} (δ_{CH_3}), 1130 cm^{-1} (γ_{CH_3} , ν_{CO} of alcohol group), 1096 cm^{-1} (ν_{CO} of alcohol group), and 1044 cm^{-1} (ν_{C-CH_3})³⁶.

Thermal properties of ESO/OLA copolymers as PSAs

Glass transition temperature indicates the temperature below which the adhesive becomes

glassy and brittle and therefore unable to form an adhesion bond. The T_g of PSA must be at least 25–45 °C below usage temperature to possess sufficient tackiness, and the T_g needs to be as broad as possible to maximize viscoelastic dissipation at the low-modulus end of glass transition³⁷. Because this research is targeting PSAs for general applications (e.g., room-temperature PSAs), the preferred T_g should be -20 to 0 °C. If the T_g of the PSA is too low, the PSA may tend to be too soft and have poor cohesion at room temperature; if the T_g is too high, the PSA may be too firm and may exhibit inadequate deformability and tack. From this point of view, copolymers from ESO with OLA3, OLA5, and OLA7 met the T_g requirement as PSAs, whereas the T_g of OLA9 copolymers was slightly out of the proper range (Figure 6, Table 2). Although a lower T_g is a prerequisite for a PSA material, T_g alone does not guarantee a material to be PSA and could not provide all the necessary information about the adhesive performance³⁸. Other factors that affect PSA performance include molecular weight, molecular architecture, supramolecular structure, and formulation.³⁷

Cationically UV-polymerized ESO homopolymer had a T_g of -14.3 °C³⁹, which is above the T_g of OLA3 (-24.3 °C) but below that of OLA5 (-4.3 °C), OLA7 (2.8 °C), and OLA9 (8.9 °C) (Table 1). Consequently, OLA3 copolymers had the lowest T_g of -15 °C to -21 °C (Table 2). The T_g first increased then decreased as the molar ratios of OLA3 to ESO increased from 2.5 (OLA3P1) to 3 (OLA3P2), then to 3.5 (OLA3P3). OLA3 mainly acted as a ring-opening agent to form polymer backbones at lower molar ratios (i.e., OLA3P1, OLA3P2). When the amount of OLA3 became excessive in the formulation relative to epoxides (i.e., OLA3P3), more chain transfer reactions occurred with OLAs during ring-opening polymerization, resulting in lower molecular weight of copolymers,

thus lower T_g . Moreover, remnant OLA3-free oligomers after polymerization would act as plasticizers for the polymer matrix, also leading to lower T_g . Overall, T_g of copolymers increased gradually as OLA chain length increased because of the higher T_g of longer chain-length OLAs. The T_g of copolymers based on OLA9 (i.e., OLA9P1, OLA9P2, OLA9P3) were 0.9 °C through 5.2 °C, which are unacceptable for room-temperature PSA applications, although the glass transition range (ΔT_g , equal to $T_{g,end} - T_{g,onset}$) of OLA9 copolymers is broader than that of the others (Table 2). T_g values of the copolymers were inconsistent with their adhesive mechanical performances as tested at room temperature, which will be discussed in the next section.

All the copolymers were thermally stable until 200 °C (Figure 7), but upon further heating, the copolymers started losing weight gradually, exhibiting $T_{d,max}$ of 380–430 °C. The thermal stability of these copolymers was comparable to some acrylic PSAs; for example, Pak and coworkers reported that an acrylic PSA decomposed rapidly above 220 °C⁴⁰. Pang et al. found that a UV-cured PSA showed a $T_{d,max}$ around 400. °C⁴¹

Mechanical performances of ESO/OLA copolymers as PSAs

Tack, peel, and shear resistance are three fundamental and interconnected physical properties of PSAs⁴². Tack value shows the ability of adhesives to wet the adherend instantaneously. Peel strength indicates the maximal forces required to remove adhesives from the adherend (i.e., adhesion). Shear resistance reveals the ability of adhesives to resist flow or creep under an applied load (cohesion). The peel, tack, and shear values of ESO homopolymers were all zero, as reported in our previous paper³⁹, indicating that the homopolymer had no tacky or adhesion functions. Most ESO/OLA copolymers exhibited

excellent adhesive performances (i.e., tack, peel, and shear resistance), and the properties varied with the chain length and amount of OLAs (Table 2). OLA3P1 with an OLA3 to ESO molar ratio of 2.5 had peel strength of 1.6 N/cm, tack of 1.7 N/cm, and shear resistance larger than 30,000 minutes. Increasing the amount of OLA3 relative to ESO from 2.5 to 3 and 3.5 increased the peel strength and tack of OLA3P2 and OLA3P3, but the shear resistance was reduced dramatically (<3,000 mins). Cohesive failure (CF) also was observed for OLA3P3. CF means some adhesive residue remained on the stainless-steel panel after peel testing, which is not desirable for repositionable PSAs. A similar trend for adhesive performance was observed for OLA5-based copolymers, which exhibited peel, tack, and shear values relatively larger than OLA3-based copolymers with the same OLA to ESO molar ratio. Some CF was observed for OLA5P2 and OLA5P3.

The excellent adhesive performance of ESO/OLA copolymers compared with ESO homopolymers was attributed to their specific macromolecular structure. First, the polymer backbone was flexible enough to meet the prerequisite of T_g for tacky polymers. Second, through the ring-opening reaction with bifunctional OLAs, extra polar groups, including unreacted $-\text{COOH}$ groups, $-\text{OH}$ groups of OLAs, and newly formed $-\text{OH}$ groups during epoxide ring-opening were introduced into the polymer system. The polar $-\text{COOH}$ and $-\text{OH}$ groups could improve wetting on the stainless steel testing panel and accelerate the rate of bond establishment and development via the formation of hydrogen bonding and other noncovalent interactions¹⁵; however, when the amount of OLAs in the resins exceeds the critical ratio, excessive chain transfer reactions occurred with OLAs during ring-opening polymerization, resulting in lower-molecular-weight polymers and weak polymer cohesion strength and cohesive failure of adhesives⁴².

Peel and shear values of OLA7-based copolymers were reduced greatly compared with OLA5-based copolymers (Table 2). An exception was noticed for OLA7P3, which was delaminated from PET backing during peel and tack testing, resulting in large variation in peel value. Therefore, the data for OLA7P3 were not necessarily comparable with the others. Peel, tack, and shear values of OLA9-based copolymers were further reduced, and the copolymer coatings were obviously inflexible during testing. Although OLA7- and OLA9-based copolymers also contained a large amount of the $-\text{COOH}$ and $-\text{OH}$ group, the T_g of these copolymers was close to or above $0\text{ }^\circ\text{C}$. The polymers were nearly glassy in the testing environment (i.e., room temperature) and were unable to wet the adherend sufficiently, so most adhesive mechanical values were very low. Based on adhesive performances, copolymers with relatively shorter-chain OLAs (i.e., OLA5, OLA3) are more desirable for PSA applications.

Viscoelasticity of ESO/OLA copolymers as PSAs

Adhesion behaviors of PSAs are strongly dependent on their viscoelastic properties. According to Dahlquist's criterion, a PSA must have a plateau modulus lower than 3.3×10^5 Pa to be able to wet the substrate and exhibit tack during bonding^{43,44}. Correlations between tack, shear or peel adhesion behaviors, and viscoelastic responses to oscillatory frequency sweeps have been well demonstrated in the literature^{45, 46}. The viscoelastic information at low frequency (~ 0.01 rad/s) describes the bond formation, whereas that at high frequency (~ 100 rad/s) describes the behavior of debonding⁴⁷. Shear performance can be correlated with G' at 0.01 rad/s (the plateau modulus). Generally, the higher the G' (0.01 rad/s) and the more extended the plateau (i.e., the difference between G' at 0.01

and 100 rad/s is smaller), the better the shear. Peel performance depends on both the bonding efficiency (G' at 0.01 rad/s) and debonding resistance (G' and G'' at 100 rad/s)⁴⁷. The lower the G' (0.01 rad/s), the more favorable the bonding, and the higher the peel strength. Furthermore, G' at 100 rad/s indicates the cohesive strength of adhesive, and G'' at 100 rad/s shows the energy of dissipation; therefore, the higher the G' (100 rad/s) and G'' (100 rad/s), the higher the peel strength. Similar to peel correlation, tack performance also depends on the bonding efficiency and debonding resistance (G' and G'' at 100 rad/s), except that the bonding frequency during tack measurement was about 1 rad/s rather than 0.01 rad/s⁴⁷.

The plateau modulus (G' at 0.01 rad/s) of all ESO/OLA copolymers was below 3.3×10^5 Pa (Dahlquist's criterion) (Figure 8, A-D), which met the prerequisite for PSAs. The G' (0.01 rad/s) of OLA3P1, OLA3P3, and OLA3P2 were 81245, 2565, and 1604 Pa, respectively (Figure 8A), which is in good agreement with their respective shear resistance of >30000, 3047, and 1740 minutes (Table 2). In addition, the difference between G' at 0.01 and 100 rad/s of OLA3P1 was much smaller than that of OLA3P2 and OLA3P3, which shows a higher degree of entanglement of the polymer, further contributing to the excellent shear resistance of OLA3P1. Similar good correlations of shear resistance values with respective G' (0.01 rad/s) values were also observed for OLA5-, OLA7-, and OLA9-based copolymers (Figure 8, B-D). Peel strength was determined by both G' at 0.01 rad/s and G' and G'' at 100 rad/s. Compared with OLA3P1, OLA3P2 and OLA3P3 had similar G'' (100 rad/s) but much smaller G' (0.01 rad/s) (Figure 8A), which favored bonding efficiency and corresponded to their obviously higher peel strength, although the G' (100 rad/s) of OLA3P1 was larger. The G' (100

rad/s) and G'' (100 rad/s) values of OLA5P1, OLA5P2, and OLA5P3 were close; however, their G' (0.01 rad/s) were 65860, 4341, and 16990 Pa, respectively (Figure 8B), which conforms to the peel strength of 2.7, 5.8, and 4.9 N/cm (Table 2). The tack of OLA-based copolymers also correlated well with their respective G' at 1 rad/s and G' and G'' at 100 rad/s.

Crosslink density (v_e) and molecular weight between crosslinks (M_c) of selected copolymers were obtained from DMA data (Figure 9). For the same oligomer, higher OLA to ESO ratio, thus higher hydroxyl and carboxyl to epoxide molar ratio, led to smaller v_e and larger M_c (Table 3). For example, OLA3P1, where the hydroxyl and carboxyl to epoxide molar ratio was 1.16, had a crosslink density of 562.9 mol/m³, while the crosslink density of OLA3P2 with hydroxyl and carboxyl to epoxide molar ratio of 1.39 was greatly reduced to 36.9 mol/m³. This is because higher amount of OLA relative to epoxide resulted in more chain transfer reactions of epoxies with hydroxyl and carboxyl groups from OLA during ring-opening polymerization, leading to lower crosslink density. Also, at the same OLA to ESO molar ratio, longer chain OLA led to copolymers with lower crosslink density than that from shorter chain OLA (e.g., 562.9 mol/m³ for OLA3P1 vs. 222.7 mol/m³ for OLA5P1). Gel content of some copolymers was listed in Table 3. As expected, higher crosslink density corresponded to higher gel content. For example, OLA3P1 had a gel content of 64.2%, while OLA3P3 had a gel content of 39.8%.

Conclusions

Thermally stable OLAs with DP of 3-9 and T_g of -24–9 °C were synthesized, and ESO/OLA copolymers were developed via an environmentally friendly UV polymerization approach. Glass transition temperature, peel strength, tack strength, shear resistance, and viscoelasticity revealed that copolymers based on relatively short-chain OLAs and moderate OLA to ESO ratios were more suitable as PSAs. The adhesion nature of the copolymers was attributed to their specific macromolecular structure, such as flexibility, internal strength, introduction of extra polar groups including –COOH and –OH in the network, and appropriate viscoelasticity at bonding and debonding frequencies. In conclusion, the ESO/OLA copolymers are excellent candidates for nearly hundred percent biobased PSAs for general-purpose tapes and labels.

Acknowledgements

This is contribution no. 15-094-J from the Kansas Agricultural Experimental Station. Financial support was provided by the USDA-NIFA Biomass Research and Development Initiative program (Grant No. 2012-10006-20230) and the Kansas Soybean Commission/United Soybean Board.

References

1. J. Johnston, *Pressure sensitive adhesive tapes: A guide to their function, design, manufacture, and use*, Pressure Sensitive Tape Council, Northbrook, IL, 2003.
2. M. F. Tse and L. Jacob, *The Journal of Adhesion*, 1996, **56**, 79-95.
3. *US Patent 3607370 Pat.*, 1971.
4. E. Cohen, O. Binshtok, A. Dotan and H. Dodiuk, *Journal of Adhesion Science and Technology*, 2012, 1-16.

5. S. Bunker, C. Staller, N. Willenbacher and R. Wool, *International Journal of Adhesion and Adhesives*, 2003, **23**, 29-38.
6. J. Shin, M. Martello, M. Shrestha, J. Wissinger, W. Tolman and M. Hillmyer, *Macromolecules*, 2011, **44**, 87-94.
7. G. Lligadas, J. C. Ronda, M. Galià and V. Cádiz, *Materials Today*, 2013, **16**, 337-343.
8. M. Alpaslan and H. Gunduz, *Nahrung-Food*, 2000, **44**, 434-437.
9. V. Sharma and P. P. Kundu, *Progress in Polymer Science*, 2006, **31**, 983-1008.
10. M. Desroches, M. Escouvois, R. Auvergne, S. Caillol and B. Boutevin, *Polymer Reviews*, 2012, **52**, 38-79.
11. Y. Xia and R. C. Larock, *Green Chemistry*, 2010, **12**, 1893-1909.
12. M. A. R. Meier, J. O. Metzger and U. S. Schubert, *Chemical Society Reviews*, 2007, **36**, 1788-1802.
13. S. P. Bunker and R. P. Wool, *Journal of Polymer Science Part a-Polymer Chemistry*, 2002, **40**, 451-458.
14. C. M. Klapperich, C. L. Noack, J. D. Kaufman, L. Zhu, L. Bonnaillie and R. P. Wool, *Journal of Biomedical Materials Research Part A*, 2009, **91A**, 378-384.
15. A. Li and K. Li, *RSC Advances*, 2014, **4**, 21521-21530.
16. C. A. Koch, P. Mallya and C. R. Williams, Google Patents, 2012.
17. C. A. Koch, Google Patents, 2010.
18. B. K. Ahn, S. Kraft, D. Wang and X. S. Sun, *Biomacromolecules*, 2011, **12**, 1839-1843.
19. B. K. Ahn, J. Sung, N. Kim, S. Kraft and X. S. Sun, *Polymer International*, 2013, **62**, 1293-1301.
20. Y. H. Li and X. S. Sun, *Journal of the American Oil Chemists' Society*, 2014, **91**, 1425-1432.
21. F. Achmad, K. Yamane, S. Quan and T. Kokugan, *Chemical Engineering Journal*, 2009, **151**, 342-350.
22. F. Codari, D. Moscatelli, G. Storti and M. Morbidelli, *Macromolecular Materials and Engineering*, 2010, **295**, 58-66.
23. ASTM D3330/D3330M-04(2010), ASTM International, West Conshohocken, PA, 2010.
24. ASTM D6195-03(2011), ASTM International, West Conshohocken, PA, 2011.
25. ASTM D3654/D3654M-06(2011), ASTM International, West Conshohocken, PA, 2011.
26. K. P. Menard, *Dynamic Mechanical Analysis: A Practical Introduction*, Taylor & Francis, 1999.
27. R. Vendamme and W. Eevers, *Macromolecules*, 2013, **46**, 3395-3405.
28. Y.-K. Chen, Y.-F. Lin, Z.-W. Peng and J.-L. Lin, *The Journal of Physical Chemistry C*, 2010, **114**, 17720-17727.
29. Y. Li and X. Sun, *Biomacromolecules*, 2010, **11**, 1847-1855.
30. F. D. Kopinke, M. Kopinke, K. Remmler, M. Mackenzie, O. Mäder and Wachsen, *Polymer degradation and stability*, 1996, **53**, 329-342.
31. K. Takizawa, H. Nulwala, J. Hu, K. Yoshinaga and C. J. Hawker, *Journal of Polymer Science Part A: Polymer Chemistry*, 2008, **46**, 5977-5990.
32. H. Dai, L. Yang, B. Lin, C. Wang and G. Shi, *Journal of the American Oil Chemists' Society*, 2009, **86**, 261-267.
33. Y. H. Hu, Y. Gao, D. N. Wang, C. P. Hu, S. Zu, L. Vanoverloop and D. Randall, *Journal of Applied Polymer Science*, 2002, **84**, 591-597.
34. G. Mashouf Roudsari, A. K. Mohanty and M. Misra, *ACS Sustainable Chemistry & Engineering*, 2014, **2**, 2111-2116.
35. R. Raghavachar, G. Sarnecki, J. Baghdachi and J. Massingill, *Journal of Coatings Technology*, 2000, **72**, 125-133.

36. G. Cassanas, M. Morssli, E. Fabrègue and L. Bardet, *Journal of Raman Spectroscopy*, 1991, **22**, 409-413.
37. C. Creton, *Mrs Bulletin*, 2003, **28**, 434-439.
38. Z. Czech and A. Butwin, *Journal of Adhesion Science and Technology*, 2009, **23**, 1689-1707.
39. Y. Li, D. Wang and X. S. Sun, *Journal of the American Oil Chemists Society*, 2015, **92**, 121-131.
40. S. Pak, J. Jiao and T. Gall, Pressure sensitive adhesive requirements for automotive electronics applications, Accessed 07/31, <http://www.pstc.org/files/public/Rak.pdf>.
41. B. Pang, C.-M. Ryu and H.-I. Kim, *Materials Science and Engineering: B*, 2013, **178**, 1212-1218.
42. Z. Czech, *Journal of Adhesion Science and Technology*, 2007, **21**, 625-635.
43. H. Yang and E. Chang, *Trends in Polymer Science*, 1997, **5**, 380-384.
44. C. A. Dahlquist, Tack, University of Nottingham, England, 1966.
45. D. Satas, *Handbook of Pressure Sensitive Adhesive Technology*, Satas & Associates, 1999.
46. E. P. Chang, *The Journal of Adhesion*, 1997, **60**, 233-248.
47. E. P. Chang, *The Journal of Adhesion*, 1991, **34**, 189-200.

Table 1. Molecular weight (MW), degree of polymerization (DP), glass transition temperature (T_g), and decomposition temperature ($T_{d,max}$) of lactic acid oligomers (OLA).

Sample	MW ^a	DP	T_g , °C	ΔC_p , J/(g·°C)	$T_{d,max}$, °C
OLA3	259.8±0.5	3.4	-24.3	0.63	278.2/375.2
OLA5	398.1±0.5	5.3	-4.3	0.74	290.0/378.6
OLA7	567.8±1.1	7.6	2.8	0.63	309.2/382.3
OLA9	674.1±1.7	9.1	8.9	0.67	330.2/382.3

Note: ^a values after ± symbol are indications of standard deviation.

Table 2. Thermal properties and PSA performance of ESO/OLA copolymers

Sample ^a	T_g , °C	ΔT_g , °C ^b	ΔC_p , J/(g·°C)	$T_{d,max}$, °C	Peel strength, N/cm	Tack strength ^c , N/cm	Shear ^e , minutes
OLA3P1	-18.2	11.6	0.54	413.9	1.6±0.1	1.7±0.1	>30,000
OLA3P2	-15.1	12.4	0.57	405.7	3.8±1.1	8.0±1.7	1,740±250
OLA3P3	-20.9	12.7	0.64	416.7	3.6±0.6 ^c	3.5±0.4	3,047±540
OLA5P1	-9.6	14.1	0.65	410.5	2.7±0.4	2.7±0.9	>30,000
OLA5P2	-13.5	13.5	0.63	399.2	5.8±0.7 ^c	7.6±0.5	12,259±585
OLA5P3	-10.8	13.8	0.65	422.7	4.9±0.2 ^c	5.9±0.3	12,105±354
OLA7P1	-3.6	23.4	0.56	392.0	0.9±0.5	2.7±0.4	6,477±513
OLA7P2	-3.3	13.4	0.59	396.9	1.5±1.0	6.8±1.1 ^c	47±15
OLA7P3	-0.2	13.4	0.56	394.1	5.5±3.6 ^{cd}	6.7±0.7 ^{cd}	35±10
OLA9P1	0.9	19.6	0.59	384.1	0.7±0.3	0.6±0.1	1,024±126
OLA9P2	5.2	18.8	0.67	427.6	0.2±0.1	0.2±0.1	1,150±112
OLA9P3	1.4	18.3	0.62	402.5	1.2±0.7 ^d	0.3±0.1	214±25

Note: ^aOLA3P1, OLA3P2, and OLA3P3 indicate the copolymer was synthesized based on OLA3 to ESO mole ratios of 2.5, 3, and 3.5, respectively. Others were designated similarly. ^b $\Delta T_g = T_{g,end} - T_{g,onset}$. ^ccohesive failure; ^ddelaminated from backing; ^evalues after ± symbol are indications of standard deviation.

Table 3. Crosslink density (v_e), molecular weight between crosslinks (M_c), and gel content of selected copolymers.

Sample	$v_e, \text{mol/m}^3$	$M_c, \text{g/mol}$	Gel content, %
OLA3P1	562.9	1954.3	64.2±0.9
OLA3P2	36.9	29782.4	39.8±3.4
OLA5P1	222.7	4939.5	50.0±1.7

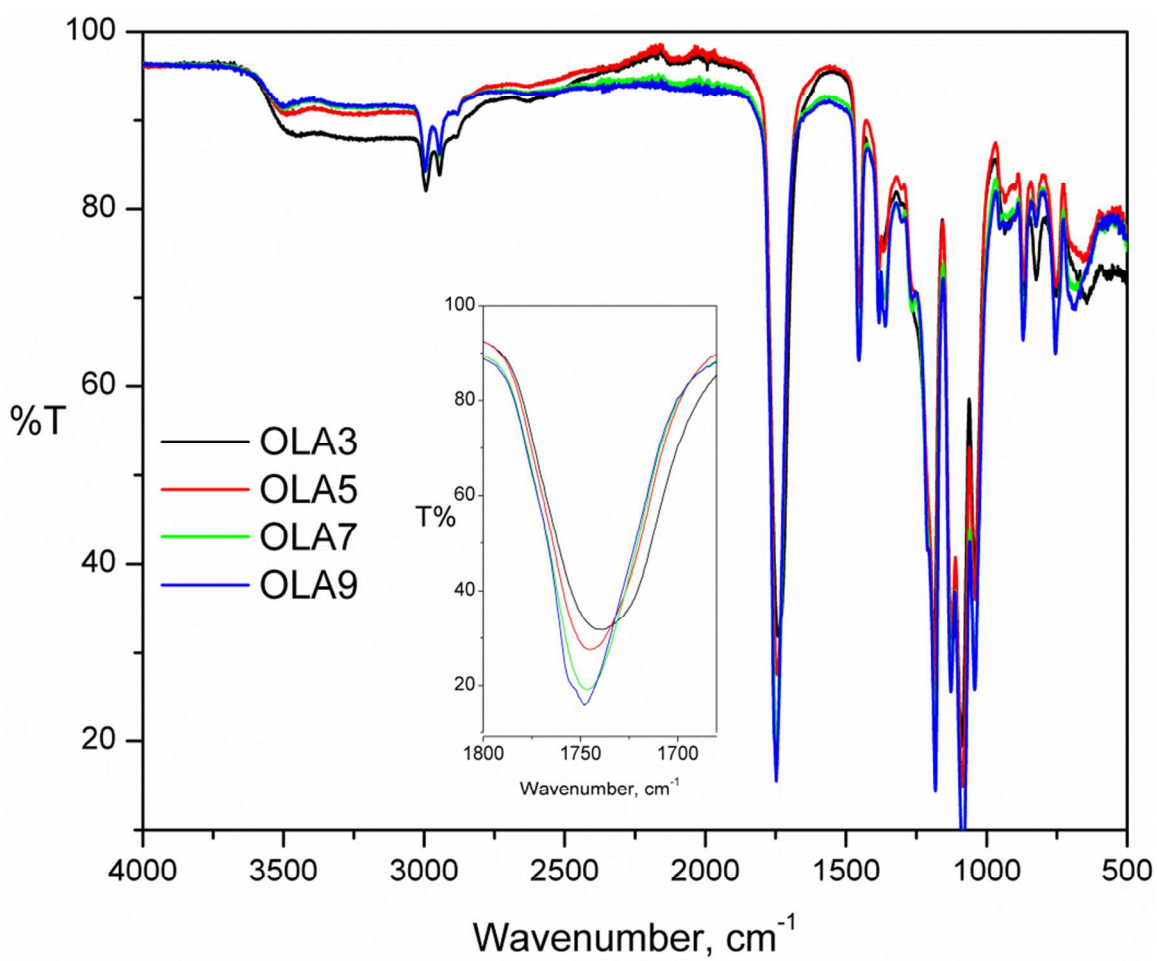


Figure 1. FTIR spectra of OLA3, OLA5, OLA7, and OLA9.

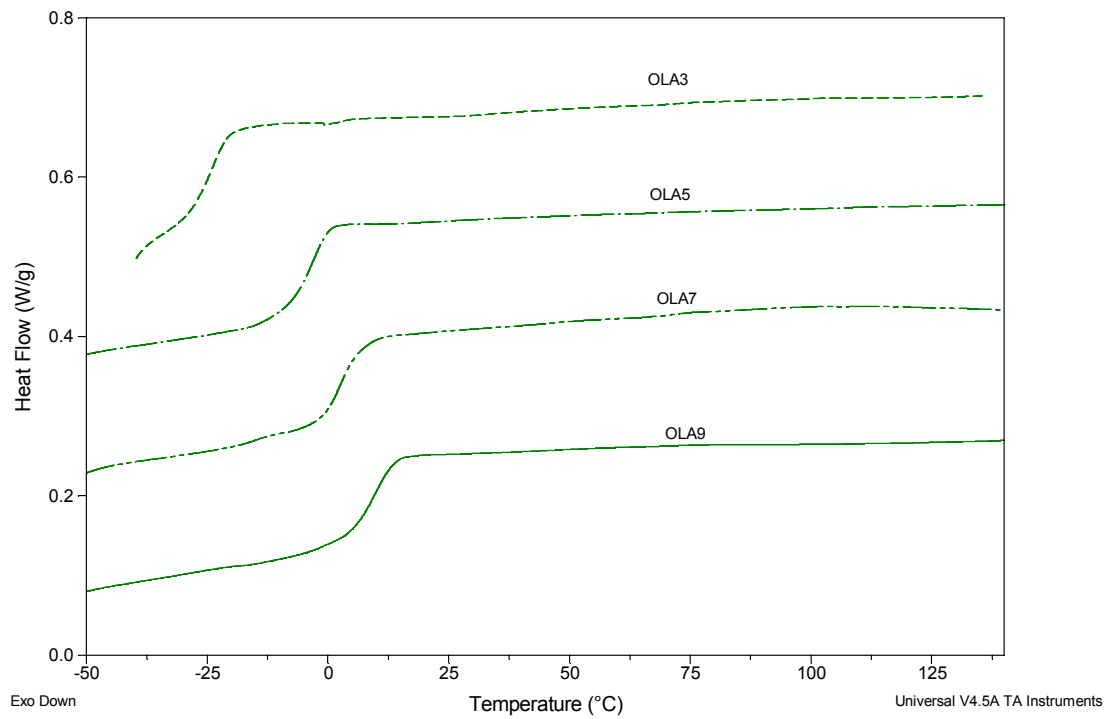


Figure 2. DSC thermograms of OLA3, OLA5, OLA7, and OLA9.

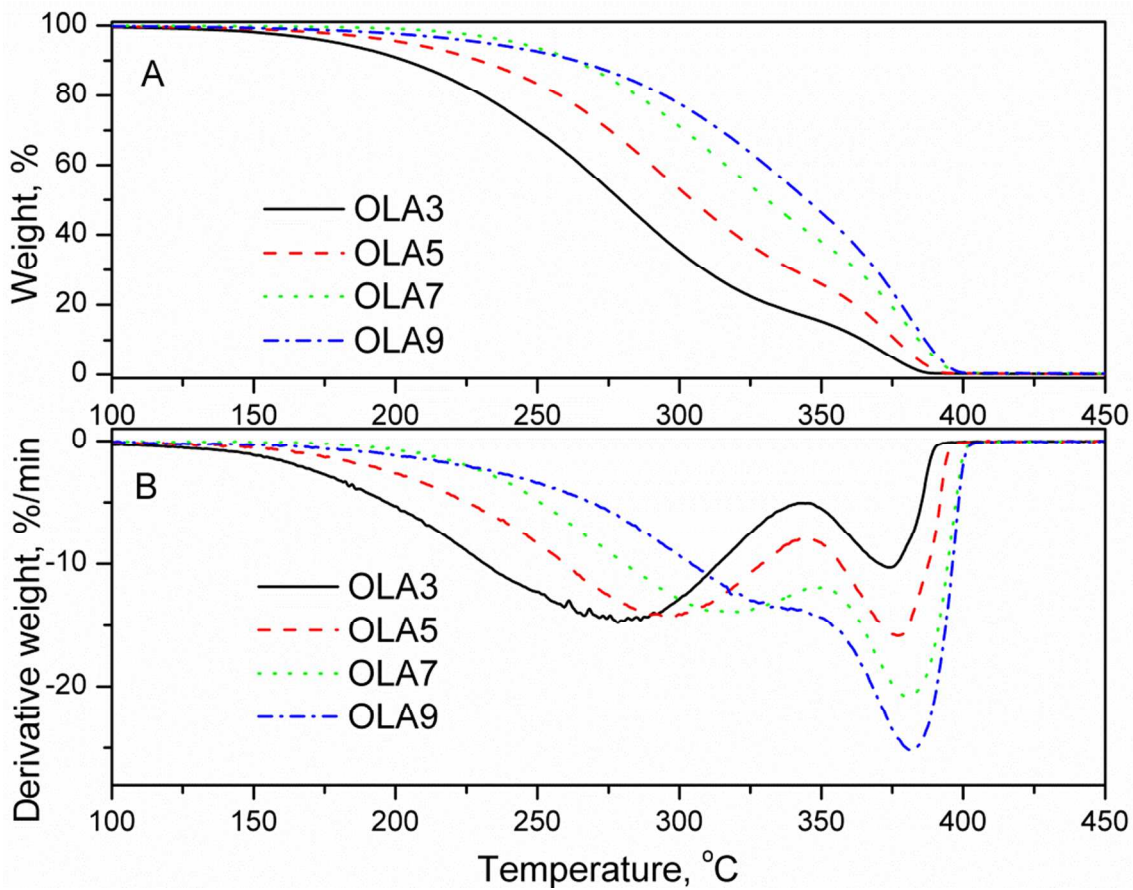


Figure 3. TGA (A) and derivative TGA (B) thermograms of OLA3, OLA5, OLA7, and OLA9.

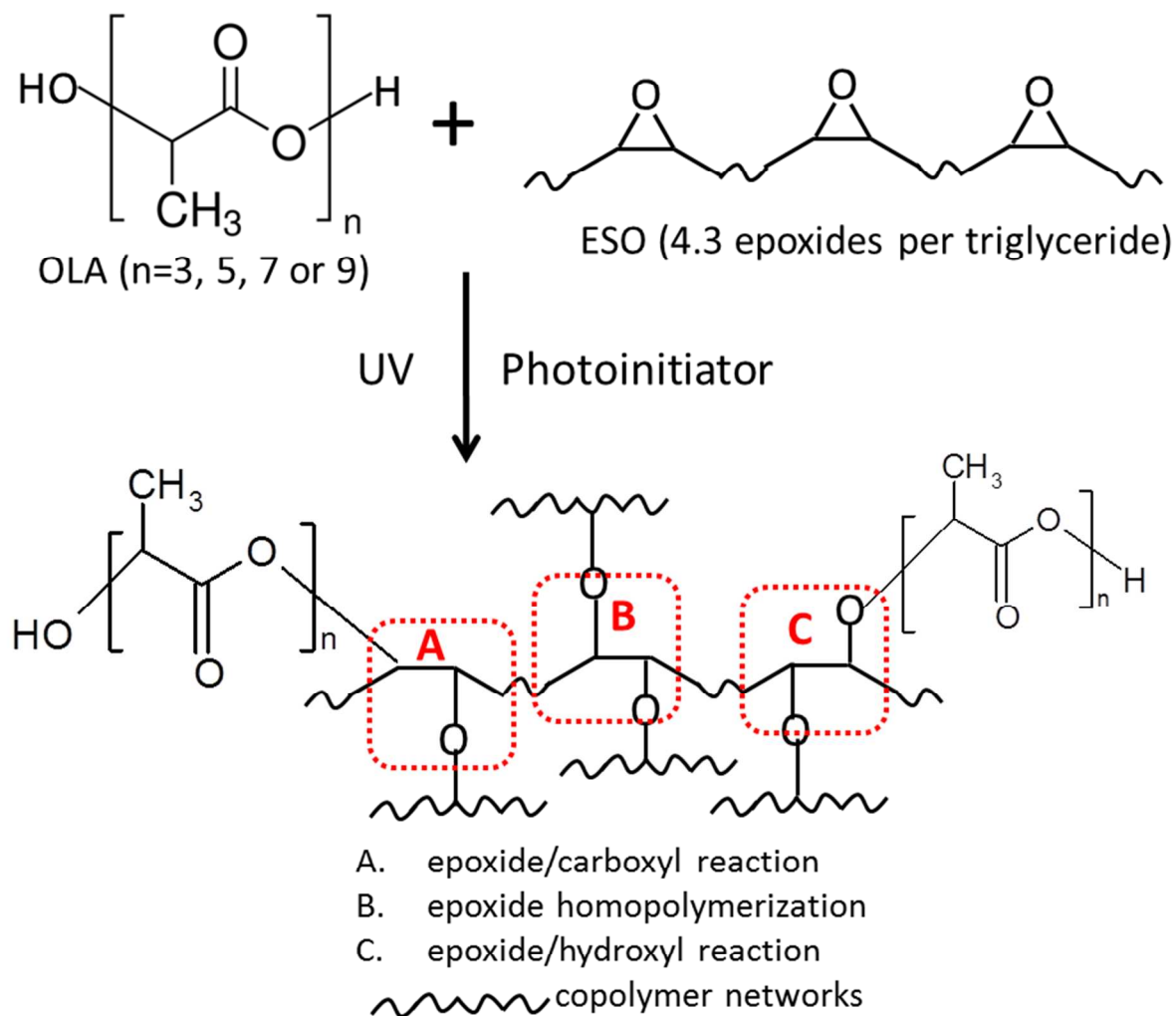


Figure 4. Synthesis pathway of ESO/OLA copolymers.

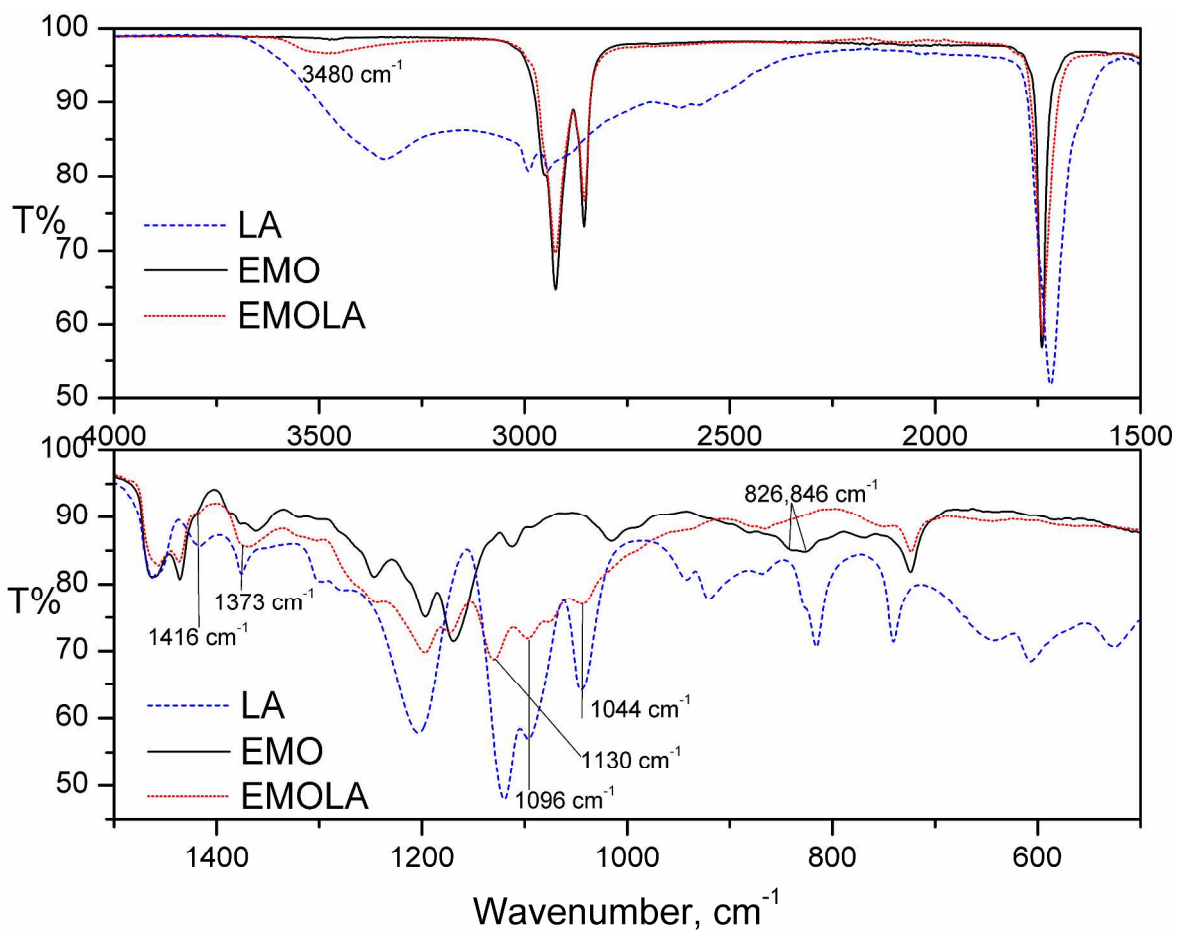


Figure 5. FTIR spectra of LA, EMO, and EMOLA.

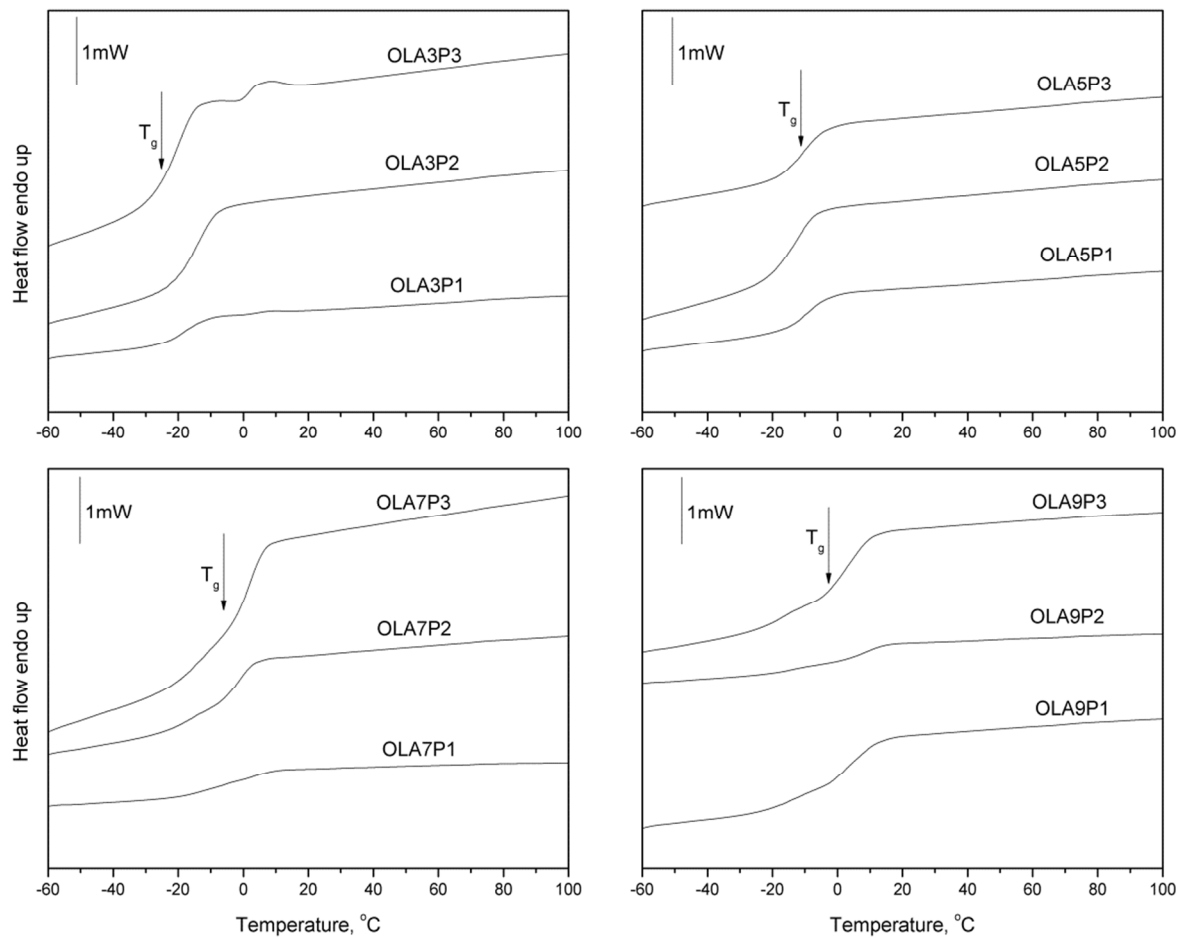


Figure 6. DSC thermograms of ESO/OLA copolymers.

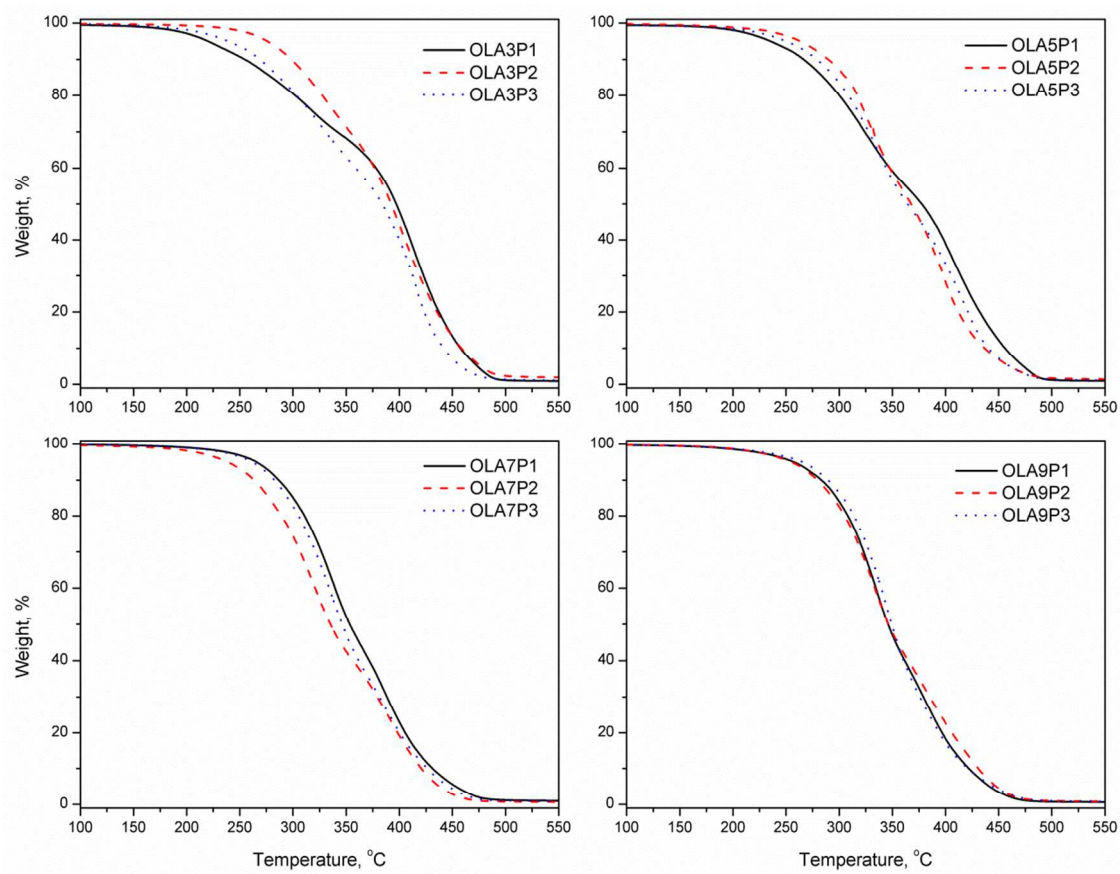
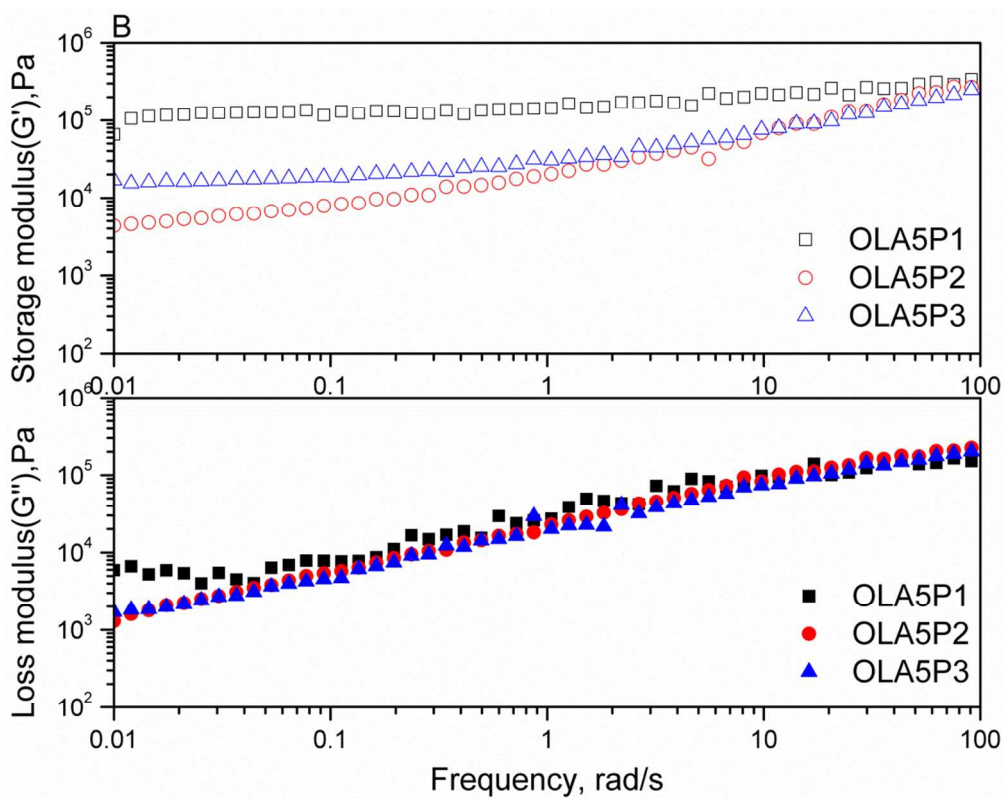
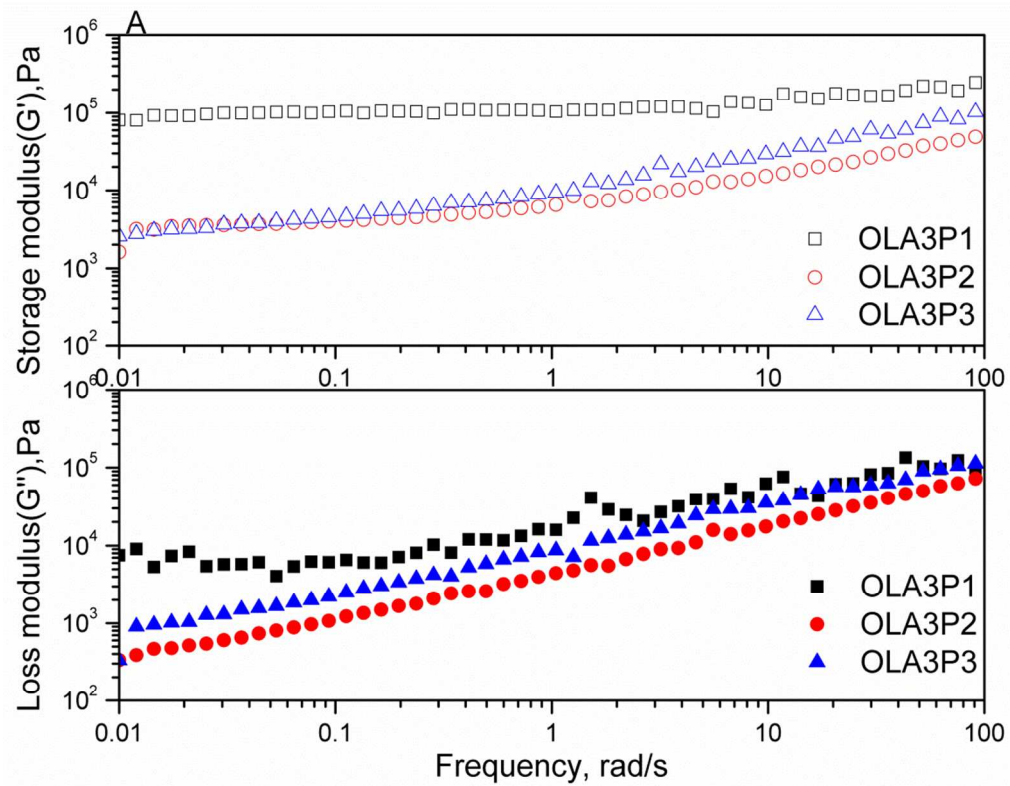


Figure 7. TGA thermograms of ESO/OLA copolymers.



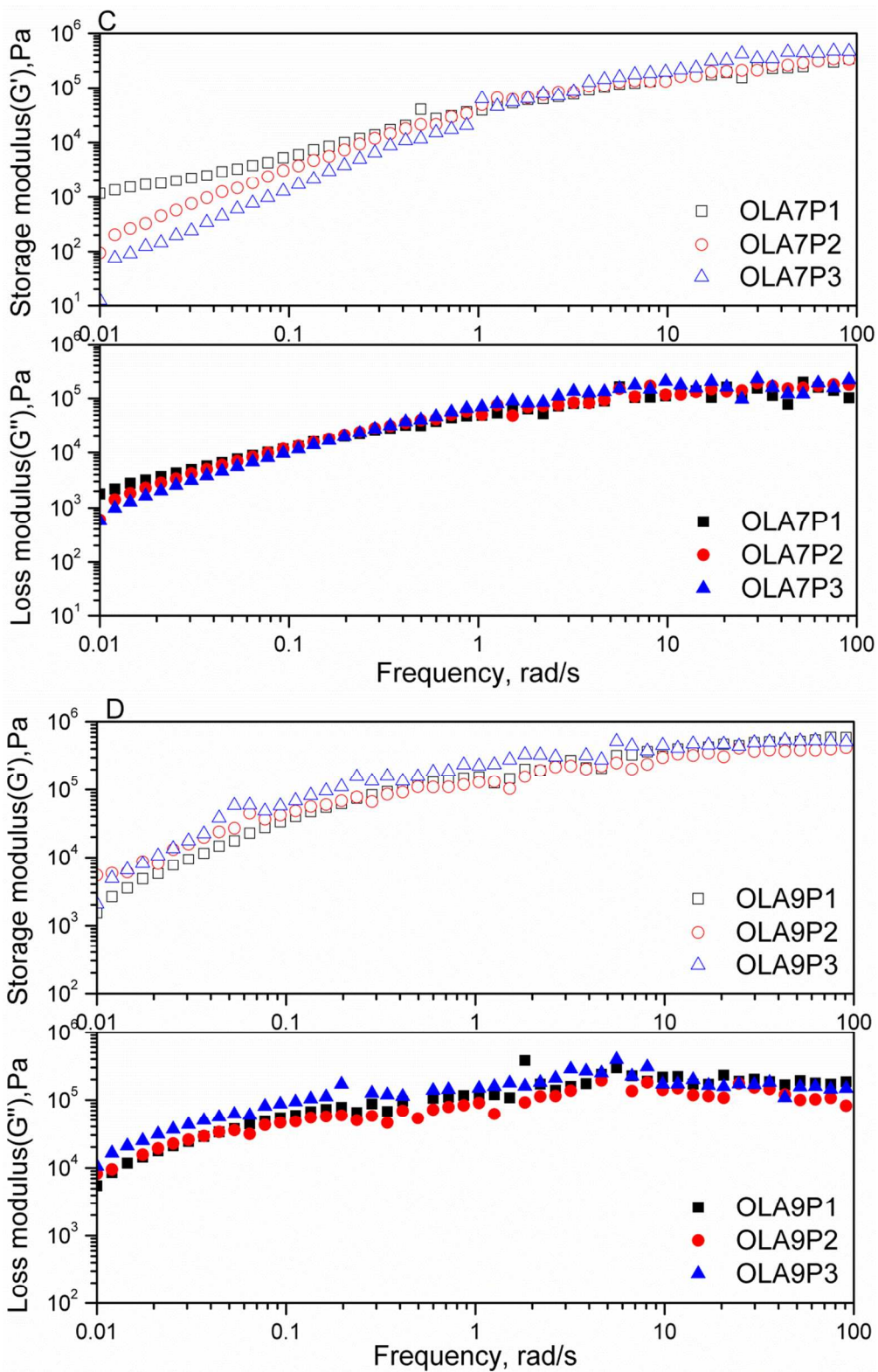


Figure 8. Frequency sweep of ESO/OLA copolymer PSAs (A-D).

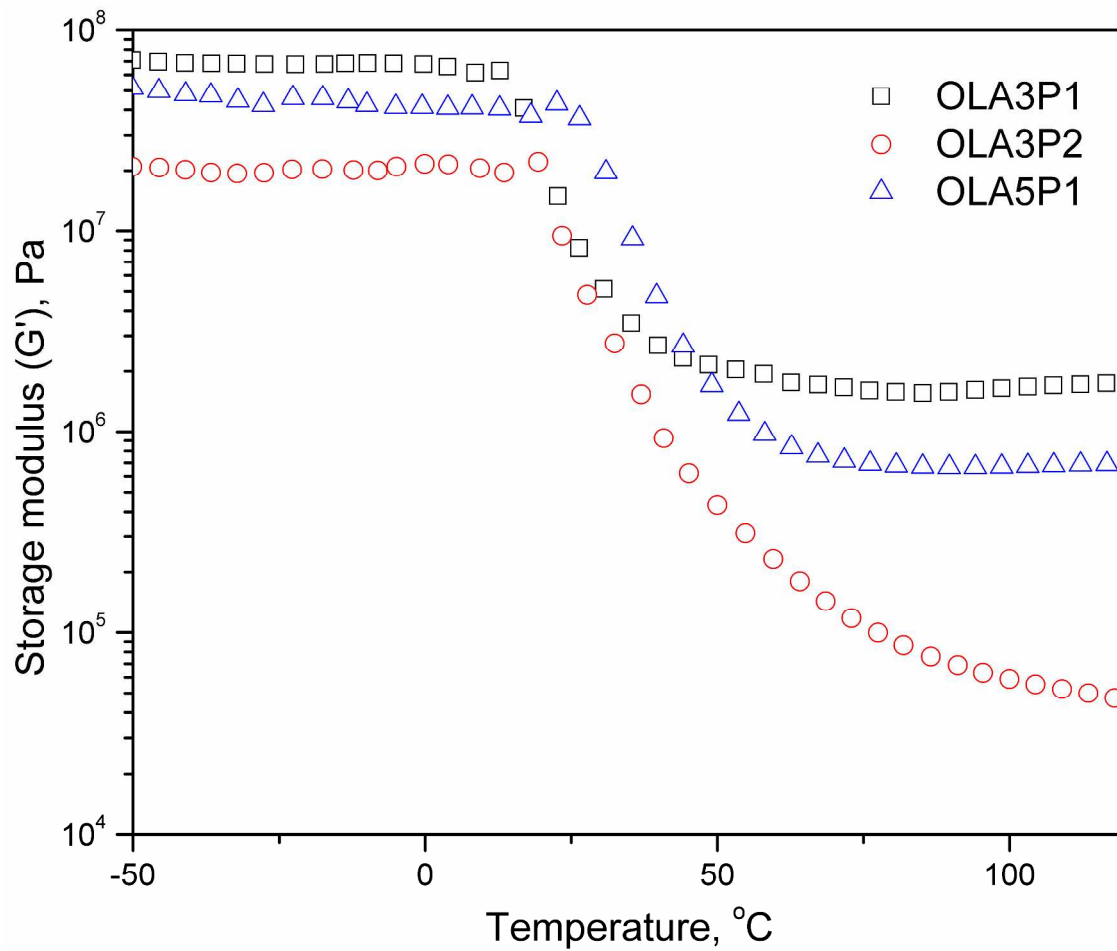


Figure 9. Storage modulus vs. temperature of selected copolymers.